$W_2Cl_4(NR_2)_2(PR'_3)_2$ Molecules. 7. Preparation, Characterization, and Structures of $W_2Cl_4(NHR)_2(NH_2R)_2$ and $W_2Cl_4(NHR)_2(PMe_3)_2$ (R = *sec*-Butyl and Cyclohexyl) and $^{31}P\{^1H\}$ NMR Studies of Trans-to-Cis Isomerizations of $W_2Cl_4(NHR)_2(PMe_3)_2$

F. Albert Cotton,* Evgeny V. Dikarev, and Wai-Yeung Wong

Department of Chemistry and Laboratory for Molecular Structure and Bonding, Texas A&M University, College Station, Texas 77843-3255

Received December 12, 1996[⊗]

Treatment of $W_2Cl_6(THF)_4$ with alkylamine NH_2R (R = Bu^s, Cy) affords a dinuclear species having the stoichiometry $W_2Cl_4(NHR)_2(NH_2R)_2$ (R = Bu^s (**1**), Cy (**2**)). This has been confirmed by single-crystal X-ray diffraction studies for **2** with the following crystal data: tetragonal space group $P\bar{4}2_1c$, a = 12.774(2) Å, c = 9.934(2) Å, Z = 2. The molecule possesses an eclipsed structure with strong N−H···Cl intramolecular hydrogen bonding, with disordering of the whole set of ligands containing the amide, amine, and chlorine ligands. Attempts have been made to treat and refine both ligand sets separately for this molecule, and the final refinement converges with reasonable bond distances and angles to R = 0.028 and $wR2$ = 0.066. In both orientations, the ligand arrangements are the same. Each W atom is surrounded by a trans set of two Cl and two N atoms with a W−W separation of 2.2884(9) Å. Substitution of the amine ligands in **1** and **2** by the monodentate phosphine PMe_3 proceeds smoothly to produce *trans*-$W_2Cl_4(NHR)_2(PMe_3)_2$ (R = Bu^s (**3**), Cy (**4**)) in high yields. In solution, both **3** and **4** readily undergo isomerization to the corresponding *cis*-$W_2Cl_4(NHR)_2(PMe_3)_2$ (R = Bu^s (**5**), Cy (**6**)). The characterization of **3**−**6** has been accomplished by IR, ^1H NMR, and $^{31}P\{^1H\}$NMR spectroscopy and mass spectrometry. The crystal data for **5** and **6** are as follows: for **5**, monoclinic space group $P2_1/a$, a = 13.339(3) Å, b = 13.446(3) Å, c = 15.179(3) Å, β = 99.33(2)°, Z = 4; for **6**, $P2_1/n$, a = 8.455(1) Å, b = 25.714(3) Å, c = 13.454(1) Å, β = 104.839(8)°, Z = 4. Each of these phosphine-containing complexes is characterized by a W_2^{6+} metal core unit and has an eclipsed $W_2Cl_4N_2P_2$ conformation. The W−W bond distances for **5** and **6** are 2.321(1) and 2.3229(5) Å, respectively, and these compounds are shown to have PMe_3 ligands cis to the amides. On the other hand, kinetic studies by $^{31}P\{^1H\}$NMR spectroscopy show that the trans-to-cis transformation in solution is an irreversible process of the first order, which is different from the reversible process observed in the case of *tert*-butyl analog. The initial rate constant was 10(1) × 10^{-3} min^{-1}, and the rate constants in the presence of excess PMe_3 were shown to be roughly constant (average 4.5 × 10^{-3} min^{-1}) over a range of [PMe_3]. These observations could be understood if, in addition to a dissociative mechanism, internal flip steps operate as a second mechanism for the process, and the flip barrier is 25−29 kcal/mol.

Introduction

In parts 1 and 2 of this series, we studied the detailed molecular structures[1] and the cis−trans isomerizations[2] of $W_2Cl_4(NHCMe_3)_2(PR'_3)_2$-type compounds ($R'_3$ = Me_3, Et_3, Pr^n_3, Me_2Ph) containing *tert*-butylamido ligands and various monodentate phosphines (**I** and **II** in Figure 1). When the fact that cis−trans isomerizations of $W_2Cl_4(NHCMe_3)_2(PR'_3)_2$ molecules might occur via unimolecular processes was recognized, and we were led to propose as a mechanism a simple internal reorientation (or internal flip) of the W_2 moiety inside the cavity formed by the eight ligand atoms,[2] our interest in further investigating this system was stimulated. We have been endeavoring to obtain additional independent and more direct evidence to support the internal flip proposal. A challenging aspect for us at this moment is to find ways to observe the remaining possible *cis* isomer of C_i symmetry (**III** in Figure 1) if the occurrence of an internal flip is to be corroborated, since isomer **III** could be obtained by a mechanism entailing only one internal flip.[2]

We have now initiated a comprehensive study aimed at further development of the chemistry of this class of compounds. One means of accomplishing this is by variation of the amido substituents or PR'_3 groups. On the basis of steric considerations, it is believed that ligands of varying steric bulk may afford new molecules of different stereochemical geometries and properties. However, previous studies revealed that changing the PR'_3 groups while keeping R = CMe_3 did not lead to promising results with regard to our goal. We therefore turned to a study of related systems with different amido groups in the hope that the unobserved *cis* isomer might be detected and even isolated. The work reported here represents the first of two papers describing our recent progress in this area. A detailed discussion of the structural and spectroscopic properties of such compounds having *sec*-butylamido or cyclohexylamido moieties will be presented in this report. Of prime importance here is the proper treatment of the disorder of the ligand sets in the structure refinement of *trans*-$W_2Cl_4(NHR)_2(NH_2R)_2$ (R =

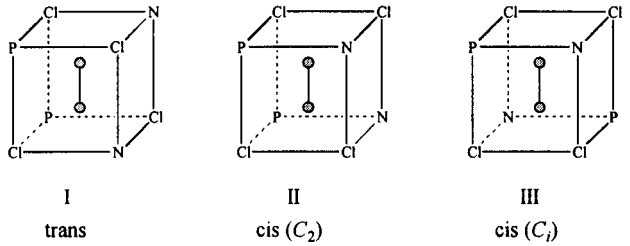

Figure 1. Three distinct isomeric forms of the $W_2Cl_4N_2P_2$ core.

[⊗] Abstract published in *Advance ACS Abstracts,* July 1, 1997.

(1) Cotton, F. A.; Yao, Z. *J. Cluster Sci.* **1994**, *5*, 11.
(2) Chen, H.; Cotton, F. A.; Yao, Z. *Inorg. Chem.* **1994**, *33*, 4255.

S0020-1669(96)01485-1 CCC: $14.00

CMe_3, Cy) molecules.[3] In addition, the results of $^{31}P\{^1H\}$ NMR studies of the trans-to-cis isomerizations for the $W_2Cl_4(NHR)_2(PMe_3)_2$ (R = Bu^s, Cy) compounds and the kinetic data for this process in the case of R = Cy will be presented.

Experimental Section

General Procedures. All reactions and manipulations of the new compounds were performed under a nitrogen or argon atmosphere on a standard double-manifold vacuum line employing Schlenk techniques and oven-dried glassware. Hexanes, toluene, and tetrahydrofuran (THF) were purified by distillation under N_2 from potassium/sodium benzophenone ketyl. Dichloromethane was distilled under N_2 from phosphorus pentoxide. Chemicals were obtained from the following sources: PMe_3, Strem Chemicals; cyclohexylamine and (±)-*sec*-butylamine, Aldrich, Inc. They were used as received. Sodium amalgam was prepared by dissolving a weighed amount of metallic sodium in an approximately measured quantity of Hg that was pumped under vacuum for at least 1 h in a Schlenk flask inside a drybox. WCl_4 was prepared by refluxing WCl_6 and $W(CO)_6$ in chlorobenzene.[4] Compounds $W_2Cl_6(THF)_4$[5] and *trans*-$W_2Cl_4(NHCMe_3)_2(NH_2CMe_3)_2$[3] were made according to the literature methods.

Syntheses. (i) *trans*-$W_2Cl_4(NHBu^s)_2(NH_2Bu^s)_2$ (1). (±)-*sec*-Butylamine (0.47 mL, 4.62 mmol) was added by syringe to a stirred solution of $W_2Cl_6(THF)_4$, prepared by reduction of WCl_4 (0.50 g, 1.54 mmol) with 1 equiv of Na−Hg (0.4%) in THF (15 mL). The solution turned gradually from greenish-yellow to orange-brown, and the reaction mixture was allowed to stir for 12 h to ensure complete reaction. The solution was then filtered through a Celite pad to remove Hg and NaCl, after which the solvent was removed *in vacuo*. The residue was thoroughly dried and then extracted with warm hexanes (20 mL). An abundant crop of orange powder of **1** was obtained upon cooling a concentrated hexanes solution to −15 °C for 1 day. Yield: 0.42 g (68% based on WCl_4). However, several attempts to get suitable single crystals for X-ray diffraction studies failed.

IR data (cm^{-1}): 3284(w), 3226(m), 1606(w), 1563(m), 1338(vw), 1301(m), 1277(m), 1262(m), 1230(w), 1192(ms), 1158(w), 1134(w), 1086(s), 1061(w), 1035(m), 1011(m), 971(vw), 926(vw), 904(w), 872-(vw), 817(m), 800(ms), 727(m).

^1H NMR data (benzene-d_6, 24 °C, δ): 0.53−1.23 (m, CH_3), 1.46 (m, CH_2), 1.66 (m, CH_2), 3.20 (m, CH), 3.65 (m, br, NH_2), 4.03 (m, CH), 4.46 (m, br, NH_2), 12.53 (d, J = 5.6 Hz, NH).

(ii) *trans*-$W_2Cl_4(NHCy)_2(NH_2Cy)_2$ (2). Procedures similar to those just described were followed to prepare *trans*-$W_2Cl_4(NHCy)_2(NH_2Cy)_2$, using cyclohexylamine (0.53 mL, 4.62 mmol) instead of *sec*-butylamine. Nicely formed orange needles of **2** (0.49 g, 70% based on 0.50 g of WCl_4) of good X-ray quality were obtained by keeping the hexanes extract at room temperature for 15 h.

IR data (cm^{-1}): 3325(m), 3268(w), 3234(m), 1619(vw), 1551(vs), 1507(vw), 1500(vw), 1340(m), 1314(vw), 1280(w), 1262(m), 1229-(w), 1207(vw), 1160(m), 1137(m), 1122(m), 1101(s), 1076(vs), 1047-(vs), 962(m), 921(vw), 890(ms), 845(ms), 805(w), 790(m), 752(ms), 712(ms), 591(m), 532(vw).

^1H NMR data (benzene-d_6, 24 °C, δ): 0.71−1.54 (m, 36H, Cy), 2.05 (m, 4H, Cy), 3.08 (m, br, 2H, NH_2), 3.69 (m, 2H, NH_2), 4.01 (m, 4H, Cy), 12.51 (d, J = 8.2 Hz, 2H, NH).

(iii) *trans*-$W_2Cl_4(NHBu^s)_2(PMe_3)_2$ (3). $W_2Cl_4(NHBu^s)_2(NH_2Bu^s)_2$ (0.50 g, 0.62 mmol) was dissolved in hexanes (15 mL), and excess PMe_3 (0.19 mL, 1.86 mmol) was added via syringe with stirring of the solution. The initial orange color turned to red within 5 min. The reaction was terminated after 0.5 h of stirring, after which the solvent, liberated *sec*-butylamine, and excess PMe_3 were removed under reduced pressure. The red product, *trans*-$W_2Cl_4(NHBu^s)_2(PMe_3)_2$ (**3**), was recrystallized from hexanes to give a homogeneous red crystalline material. Yield: 0.38 g (76%).

IR data (cm^{-1}): 3249(sh), 3238(w), 1420(w), 1367(m), 1298(m), 1280(ms), 1261(s), 1146(ms), 1093(vs), 1023(s), 955(s), 863(w), 844-(w), 800(s), 734(w), 710(m), 675(vw).

^1H NMR data (benzene-d_6, 24 °C, δ): 0.88 (t, J = 7.5 Hz, CH_2CH_3), 0.90 (t, J = 7.5 Hz, CH_2CH_3), 1.19 (d, J = 6.6 Hz, $CHCH_3$), 1.23 (d, J = 6.4 Hz, $CHCH_3$), 1.40 (d, J = 8.5 Hz, PMe_3), 1.46 (m, $CHCH_2$-CH_3), 1.66 (m, $CHCH_2CH_3$), 4.02 (m, CH), 12.05 (m, br, NH).

$^{31}P\{^1H\}$NMR data (benzene-d_6, 19 °C, δ): −5.30 (s, $^1J_{W-P}$ = 116 Hz), −5.21 (s, $^1J_{W-P}$ = 116 Hz).

FAB/DIP MS (NBA, *m/z*): 806 ([M]$^+$), 769 ([M − Cl]$^+$), 729 ([M − PMe_3]$^+$), 693 ([M − Cl − PMe_3]$^+$), 654 ([M − 2PMe_3]$^+$).

(iv) *cis*-$W_2Cl_4(NHBu^s)_2(PMe_3)_2$ (5). When a solution of *trans*-$W_2Cl_4(NHBu^s)_2(PMe_3)_2$ (**3**) in isomeric hexanes was kept at room temperature, the solution became steadily darker, and after 1 week, red crystals together with some red-brown crystals of **5** were obtained at the bottom of the Schlenk tube (overall yield, 72%). A structure determination of the red-brown crystals showed this compound[6] to be polymorphic with that of the red crystals, each containing a different enantiomeric ratio of *R* and *S* configurations of $NHBu^s$ groups in a single dinuclear complex. Thus, the molecules pack in slightly different ways in these two cases, but because of poor refinement, the detailed dimensions for the red-brown polymorph will not be reported.

IR data (cm^{-1}): 3195(m), 1418(m), 1367(ms), 1342(vw), 1300(m), 1286(ms), 1280(m), 1267(m), 1142(m), 1133(vw), 1119(w), 1106(m), 1090(ms), 1034(w), 1010(w), 960(vs), 857(w), 797(m), 744(ms), 732-(ms), 673(w), 530(vw).

^1H NMR data (benzene-d_6, 24 °C, δ): 0.76 (t, CH_2CH_3), 0.81 (t, CH_2CH_3), 0.91 (d, J = 6.34 Hz, $CHCH_3$), 1.04 (d, J = 6.18 Hz, $CHCH_3$), 1.31−1.61 (m, br, $CHCH_2CH_3$), 1.44 (d, J = 9.6 Hz, PMe_3), 1.45 (d, J = 9.0 Hz, PMe_3), 3.42 (m, CH), 3.54 (m, CH), 11.88 (m, br, NH).

$^{31}P\{^1H\}$NMR data (benzene-d_6, 19 °C, δ): −2.18 (s, $^1J_{W-P}$ = 308 Hz, $^3J_{P-P}$ = 5.2 Hz), −2.15 (s, $^1J_{W-P}$ = 308 Hz, $^3J_{P-P}$ = 5.2 Hz).

FAB/DIP MS (NBA, *m/z*): 806 ([M]$^+$), 769 ([M − Cl]$^+$), 729 ([M − PMe_3]$^+$), 693 ([M − Cl − PMe_3]$^+$), 654 ([M − 2PMe_3]$^+$), 618 ([M − Cl − 2PMe_3]$^+$).

(v) *trans*-$W_2Cl_4(NHCy)_2(PMe_3)_2$ (4). The synthesis of **4** was conducted in essentially the same way as that of **3**. An orange hexanes solution of **2** (0.50 g in 20 mL) was prepared, and to this solution was added an excess of PMe_3 (0.17 mL, 1.66 mmol). This mixture was stirred at room temperature for 30 min, giving a red solution. The distillation of all volatile components under vacuum from the red solution resulted in a red residue, which was then redissolved in a minimum quantity of hexanes. A crop of bright red crystals of **4** was readily obtained in 2 days at 0 °C. Crystals grown in this way have been used for the X-ray data collection. The supernatant liquid was allowed to crystallize further at −15 °C, and a second crop of red crystalline solid was obtained, for an overall yield of 0.38 g (80%).

IR data (cm^{-1}): 3216(w), 1450(s), 1418(w), 1344(w), 1296(w), 1280(m), 1260(w), 1124(w), 1100(sh), 1079(s), 1019(w), 951(s), 889-(w), 875(vw), 848(w), 794(m), 738(m), 706(w), 672(vw).

^1H NMR data (benzene-d_6, 24 °C, δ): 1.03 (m, Cy), 1.19−1.67 (m, br, Cy), 1.39 (d, J = 8.2 Hz, 18H, PMe_3), 3.99 (m, Cy), 12.08 (d, J = 9.0 Hz, 2H, NH).

$^{31}P\{^1H\}$NMR data (benzene-d_6, 19 °C, δ): −5.37 (s, $^1J_{W-P}$ = 113 Hz).

FAB/DIP MS (NBA, *m/z*): 858 ([M]$^+$), 782 ([M − PMe_3]$^+$), 704 ([M − 2PMe_3]$^+$), 684 ([M − NHCy − PMe_3]$^+$).

(vi) *cis*-$W_2Cl_4(NHCy)_2(PMe_3)_2$ (6). A solution of *trans*-$W_2Cl_4(NHCy)_2(PMe_3)_2$ (**4**) in hexanes was allowed to stand at room temperature, and the solution gradually darkened. After a few days, black crystals of **6** (69%) were found on the wall and at the base of the Schlenk tube. Single crystals suitable for X-ray diffraction studies were readily formed by a hexane−toluene layering procedure under ambient conditions.

(3) Bradley, D. C.; Errington, M. B.; Hursthouse, M. B.; Short, R. L. *J. Chem. Soc., Dalton Trans.* **1986**, 1305.
(4) Schrock, R. R.; Sturgeoff, L. G.; Sharp, P. R. *Inorg. Chem.* **1983**, *22*, 2801.
(5) (a) Chisholm, M. H.; Eichhorn, B. W.; Folting, K.; Huffman, J. C.; Ontiveros, C. D.; Streib, W. E.; Van Der Sluys, W. G. *Inorg. Chem.* **1987**, *26*, 3182. (b) Sharp, P. R.; Schrock, R. R. *J. Am. Chem. Soc.* **1980**, *102*, 1430.

(6) Crystal data for the red-brown polymorph of *cis*-$W_2Cl_4(NHBu^s)_2(PMe_3)_2$: $W_2Cl_4P_2C_{14}H_{38}N_2$, M = 805.90, monoclinic, space group $P2_1/a$, a = 13.627(2) Å, b = 12.018(1) Å, c = 16.440(3) Å, β = 96.90(1)°, V = 2673.0(6) Å^3, Z = 4.

IR data (cm^{-1}): 3208(w), 3189(sh), 3154(vw), 1608(vw), 1583(vw), 1511(m), 1415(w), 1349(w), 1299(w), 1286(m), 1280(m), 1261(m), 1235(vw), 1221(w), 1184(vw), 1170(vw), 1139(vw), 1124(ms), 1099-(m), 1065(m), 1045(br, w), 981(w), 954(s), 890(vw), 861(vw), 850-(w), 804(w), 754(w), 748(w), 738(w), 725(w), 675(vw), 585(w).

^{1}H NMR data (benzene-d_6, 24 °C, δ): 0.94 (m, Cy), 1.32 (m, Cy), 1.48 (d, J = 10.0 Hz, 18H, PMe_3), 1.97 (m, Cy), 3.48 (m, Cy), 11.84 (br, NH).

^{31}P{^{1}H}NMR data (benzene-d_6, 19 °C, δ): −1.89 (s, $^1J_{W-P}$ = 308 Hz, $^3J_{P-P}$ = 5.0 Hz).

FAB/DIP MS (NBA, *m/z*): 858 ([M]$^+$), 821 ([M − Cl]$^+$), 782 ([M − PMe_3]$^+$), 747 ([M − Cl − PMe_3]$^+$), 704 ([M − 2PMe_3]$^+$), 684 ([M − NHCy − PMe_3]$^+$).

Physical Measurements. The IR spectra were recorded on a Perkin-Elmer 16PC FT-IR spectrophotometer as Nujol mulls between KBr plates. ^{1}H NMR spectra were obtained on a Varian XL-200 spectrometer operated at 200 MHz. Resonances were referenced internally to the residual proton impurity in the deuterated solvent. The ^{31}P{^{1}H} NMR data were obtained at room temperature on a Varian XL-200 broad-band spectrometer operated at 81 MHz and using an internal deuterium lock and 85% H_3PO_4 as an external standard. Positive chemical shifts were measured downfield from H_3PO_4/D_2O. The positive FAB/DIP (DIP = direct insertion probe) mass spectra were acquired using a VG Analytical 70S high-resolution, double-focusing, sectored (EB) mass spectrometer. Samples for analysis were prepared by dissolving the neat solid compound in *m*-nitrobenzyl alcohol (NBA) matrix on the DIP tip. The probe was then inserted into the instrument through a vacuum interlock and the sample bombarded with 8 keV xenon primary particles from an Ion Tech FAB gun operating at an emission current of 2 mA. Positive secondary ions were extracted and accelerated to 6 keV and then mass analyzed.

The kinetic measurements were carried out by ^{31}P{^{1}H}NMR spectroscopy at 40 °C with about 15 mg of *trans*-$W_2Cl_4(NHCy)_2(PMe_3)_2$ in 2.5 mL of a 1:4 mixture of C_6D_6 and C_7H_8. To each solution except one was added some additional PMe_3. Before the temperature was raised to 40 °C, spectra measured at room temperature were integrated to obtain the ratio of free to bonded PMe_3. The temperature was then raised as quickly as possible to 40 °C, and the spectra were measured at regular time intervals. Rate constants were calculated on the basis of a first-order irreversible rate law, $k = 1/t\ \ln(A_0/A_t)$.

X-ray Crystallographic Procedures. Single crystals of **2**, **5**, and **6** were obtained as described herein. The normal crystallographic procedures we followed have been presented elsewhere.[7] For **2**, **5**, and **6**, suitable crystals were fastened to the end of a glass fiber with a thin layer of epoxy resin, and intensity data were collected at ambient temperature on a Rigaku AFC5R diffractometer equipped with a rotating Cu radiation source (λ Cu Kα = 1.54184 Å). Axial lengths and Laue classes were confirmed by axial photography. The identification of the crystal systems, data collection, and structure solutions and refinements are described below for each individual crystal studied. All calculations were carried out on a DEC 3000-800 AXP workstation. Data sets were corrected for decay where necessary and for Lorentz and polarization effects. An absorption correction based on azimuthal scans of six reflections with Eulerian angle χ near 90° was applied to the data using the TEXSAN software package.[8] For all structures, the positions of W atoms were located by direct methods in the SHELXTL program.[9] The remainder of the non-hydrogen atoms were found by use of a combination of least-squares refinements and difference Fourier techniques in the SHELXL-93 structure refinement program.[10] In each model, hydrogen atoms were introduced in idealized positions for the calculations of structure factors, and the entire model was refined to convergence. Pertinent crystallographic data and refinement results for each compound are collected in Table 1. A listing of the important molecular dimensions for **2** is presented in Table 2. Selected bond distances and angles and torsion angles about the W−W bond for both **5** and **6** are shown in Table 6. Tables of positional and isotropic parameters and anisotropic displacement parameters, as well as complete tables of bond distances and angles and coordinates of hydrogen atoms, are available as Supporting Information.

Table 1. Crystallographic Data for *trans*-$W_2Cl_4(NHCy)_2(NH_2Cy)_2$ (**2**), *cis*-$W_2Cl_4(NHBu^s)_2(PMe_3)_2$ (**5**), and *cis*-$W_2Cl_4(NHCy)_2(PMe_3)_2$ (**6**)

	2	**5**	**6**
formula	$W_2Cl_4C_{24}H_{50}N_4$	$W_2Cl_4P_2C_{14}H_{38}N_2$	$W_2Cl_4P_2C_{18}H_{42}N_2$
fw	904.18	805.90	857.98
space group	$P\bar{4}2_1c$ (No. 114)	$P2_1/a$ (No. 14)	$P2_1/n$ (No. 14)
a, Å	12.782(2)	13.339(3)	8.455(1)
b, Å	12.782(2)	13.446(3)	25.714(3)
c, Å	9.943(2)	15.179(3)	13.454(1)
β, deg	90	99.33(2)	104.839(8)
V, Å^3	1624.5(5)	2686(1)	2827.5(5)
Z	2	4	4
ρ_{calc}, g/cm^3	1.848	1.993	2.015
μ, mm^{-1}	16.060	20.391	19.425
radiation (λ, Å)	Cu Kα (1.541 84)	Cu Kα (1.541 84)	Cu Kα (1.541 84)
temp, °C	20	20	20
transm factors	1.0000−0.7970	1.0000−0.3815	1.0000−0.8118
R1,[a] *wR2*[b] [$I > 2\sigma(I)$]	0.028, 0.066	0.057, 0.164	0.027, 0.064
R1,[a] *wR2*[b] (all data)	0.057, 0.078	0.064, 0.172	0.043, 0.070

[a] $R1 = \sum||F_o| - |F_c|/\sum|F_o|$. [b] $wR2 = [\sum[w(F_o^2 - F_c^2)^2]/\sum[w(F_o2)^2]]^{1/2}$.

Table 2. Selected Bond Distances (Å) and Angles (deg) for *trans*-$W_2Cl_4(NHCy)_2(NH_2Cy)_2$ (**2**)

W(1)−W(1A)	2.2884(9)	W(1)−N(1)	2.19(2)
W(1)−N(2C)	1.91(3)	W(1)−Cl(1)	2.37(2)
W(1)−Cl(2C)	2.38(1)		
N(1)−W(1)−Cl(1)	84(1)	W(1A)−W(1)−N(1)	99.2(5)
N(1)−W(1)−Cl(2C)	79.1(9)	W(1A)−W(1)−N(2C)	100.1(8)
N(1)−W(1)−N(2C)	160.2(6)	W(1A)−W(1)−Cl(1)	102.0(5)
N(2C)−W(1)−Cl(1)	97(1)	W(1A)−W(1)−Cl(2C)	102.7(4)
N(2C)−W(1)−Cl(2C)	92 (1)	W(1)−N(1)−C(1)	113(2)
Cl(1)−W(1)−Cl(2C)	151.8(3)	W(1)−N(2C)−C(1C)	128(2)

***trans*-$W_2Cl_4(NHCy)_2(NH_2Cy)_2$ (2).** A well-formed orange needle with dimensions of 0.05 mm × 0.08 mm × 0.55 mm was mounted for intensity measurements. Least-squares refinement of 25 carefully centered reflections in the range $28 < 2\theta < 53°$ resulted in a tetragonal cell. Laue symmetry 4/*mmm* was derived from oscillation photographs on *a*, *b*, *c*, and 110. Systematic extinctions uniquely determined the space group as the acentric group $P\bar{4}2_1c$. In order to determine the absolute configuration, Bijvoet pairs were collected. A total of 2742 data in the range $9 < 2\theta < 120°$ were measured using an $\omega-2\theta$ scan technique. The overall change in standard intensities during the period of data collection was −11%. Only W and Cl atoms were refined anisotropically. All other ligand atoms and the carbon atoms in cyclohexyl rings were assigned a site occupancy factor (SOF) of 0.5 each. Final refinement anisotropic for W and Cl atoms of 75 parameters and 12 restrains converged with *R* (for 779 reflections with $I > 2\sigma(I)$ of 0.028 and *R* for all 1218 data of 0.057. The highest peak in the final difference map was 0.37 e/Å^3. The absolute configuration of **2** was established by the method described by Flack (Flack *x* parameters = −0.07(8)).

***cis*-$W_2Cl_4(NHBu^s)_2(PMe_3)_2$ (5).** Crystals of *cis*-$W_2Cl_4(NHBu^s)_2(PMe_3)_2$ were obtained in two crystalline forms and were separated under a microscope on the basis of their slightly different colors and shapes (red blocks and red-brown cubes). A red block-shaped crystal of **5** having dimensions 0.13 mm × 0.15 mm × 0.25 mm was selected and mounted. Least-squares refinement of 25 reflections in the range $48 < 2\theta < 51°$ resulted in unit cell parameters having primitive monoclinic symmetry. The Laue symmetry of 2/*m* was verified by axial photographs. The diffraction data were collected at room temperature in the range $5 < 2\theta < 120°$. A total of 4189 data were

(7) Cotton, F. A.; Dikarev, E. V.; Wong, W. Y. *Inorg. Chem.* **1997**, *36*, 80.
(8) TEXSAN: Crystal Structure Analysis Package, Molecular Structure Corp., Houston, TX, 1985.
(9) SHELXTL V. 5, Siemens Industrial Automation Inc., Madison, WI, 1994.
(10) Sheldrick, G. M. In *Crystallographic Computing 6*; Flack, H. D., Parkanyi, L., Simon, K., eds.; Oxford University Press: Oxford, UK, 1993; p 111.

collected using an $\omega-2\theta$ scan motion. A plot of three representative reflections measured at regular intervals revealed that 15% of diffraction intensity was lost during the experiment. Systematic absences in the data unambiguously determined the space group to be $P2_1/a$. After anisotropic refinement of most atoms, it was apparent that one of the two amido groups was disordered. We have both *R* and *S* enantiomers (with SOF's of 0.5 each) in one of the $NHBu^s$ groups. For another polymorph,[6] there is no disorder, and both amido groups in one molecule conform to the same enantiomer. It should be noted that the total ratio of *R* to *S* in each unit cell is 0.50:0.50 for both cases. Full refinement of 207 parameters resulted in residuals *R* based on 3522 reflections with $I > 2\sigma(I)$ and *R* based on all 3989 data of 0.057 and 0.064, respectively. The largest residual peak in the final difference electron density map was 1.88 e/A^3, in the vicinity of W atoms.

***trans*-$W_2Cl_4(NHCy)_2(PMe_3)_2$ (4).** A red crystal with dimensions 0.20 mm × 0.30 mm × 0.45 mm was selected and affixed to the tip of a quartz fiber with silicone grease. The diffraction data were collected on an Enraf-Nonius CAD-4S diffractometer (λ Mo Kα = 0.710 73 Å) at −100 °C. With 25 reflections ($20 < 2\theta < 30$), the unit cell was shown to be orthorhombic, $a = 9.396(2)$ Å, $b = 17.980(4)$ Å, $c = 8.627(2)$ Å, $V = 1457.5$ Å^3, $Z = 2$. The Laue symmetry *mmm* was displayed by the axial photographs, but disorder streaks were observed on these photos. When we tried to solve the structure in the space group *Pba*2, which was justified by the systematic absences observed, and several other space groups with lower Laue symmetries as well, a disorder of the W−W vector (disorder ratio 0.50:0.50) was always found. As a consequence of this disorder, all the ligands appeared distorted. At this time, it is pretty clear that we are dealing with the *trans* isomer, but we have not yet achieved a satisfactory solution of this structure.

***cis*-$W_2Cl_4(NHCy)_2(PMe_3)_2$ (6).** A red-brown block with approximate dimensions 0.10 mm × 0.13 mm × 0.25 mm was used for intensity measurements. A primitive monoclinic cell was derived from the indexing on the basis of 25 reflections with the 2θ range of 19−37° and further confirmed by axial photos. The X-ray diffraction data were gathered at room temperature via an $\omega-2\theta$ scan method. Periodic monitoring of three representative reflections revealed no loss in crystal integrity throughout data collection. The structure was solved and refined in the monoclinic space group $P2_1/n$. After the anisotropic refinement of heavy atoms had converged, it became obvious that one cyclohexylamido group was disordered over two sites. This disorder was modeled by restraining the chemically equivalent bonds to be approximately equal. Also, the SOF's were allowed to vary but were constrained so that the sum was equal to 1. The resulting model gave reasonable bond distances and angles. All the non-hydrogen atoms were refined with anisotropic displacement parameters. Final least-squares refinement of 309 parameters led to residuals of $R = 0.027$ for 3491 reflections with $I > 2\sigma(I)$ and $R = 0.043$ for all 4212 data. A final difference Fourier map revealed that the highest remaining peak of electron density (0.78 e/Å^3) was located near W(1).

Results and Discussion

Synthesis and Properties. The dinuclear W(III)−W(III) precursors, *trans*-$W_2Cl_4(NHR)_2(NH_2R)_2$ (R = Bu^s (**1**), Cy (**2**)), used for the preparation of the $W_2Cl_4(NHR)_2(PMe_3)_2$ compounds are easily synthesized by reaction of the appropriate amines RNH_2 (R = Bu^s, Cy) with $W_2Cl_6(THF)_4$, which is formed *in situ* by the reduction of WCl_4 with Na−Hg in tetrahydrofuran[5] (eq 1). Compounds **1** and **2** can be isolated in high yields (**1**, 68%; **2**, 70%) as orange solids from orange-brown solutions. The yields are comparable to that reported in the literature for the *tert*-butyl analog.[3] These intermediate complexes, like $W_2Cl_4(NHCMe_3)_2(NH_2CMe_3)_2$, were found to adopt a trans stereochemistry. A facile substitution reaction between *trans*-$W_2Cl_4(NHR)_2(NH_2R)_2$ (**1** and **2**) and PMe_3 occurs to give *trans*-$W_2Cl_4(NHR)_2(PMe_3)_2$ (R = Bu^s (**3**), Cy (**4**)) in *ca.* 76−80% yields (eq 2). We observed that the initial substitution products

$$W_2Cl_6(THF)_4 + 6NH_2R \rightarrow W_2Cl_4(NHR)_2(NH_2R)_2 + 2[RNH_3]Cl + 4THF \quad (1)$$

$$W_2Cl_4(NHR)_2(NH_2R)_2 + 2PMe_3 \rightarrow W_2Cl_4(NHR)_2(PMe_3)_2 + 2NH_2R \quad (2)$$

are pure *trans* isomers, and thus stereochemistry is preserved upon substitution of NHR_2 by PMe_3. However, the *trans*-$W_2Cl_4(NHR)_2(PMe_3)_2$ compounds **3** and **4** isomerize readily and completely in solution to *cis*-$W_2Cl_4(NHR)_2(PMe_3)_2$ (R = Bu^s (**5**), Cy (**6**)). The major difference here compared with the *tert*-butyl case[2] is that the isomerization is found to be complete and irreversible in the present two cases, whereas an equilibrium is reached when NHR is $NHCMe_3$.

These new metal−metal-bonded complexes are readily soluble in aromatic solvents such as benzene and toluene, but only complexes **1**−**4** exhibit good solubility in aliphatic hydrocarbons. It should be noted that they all display rather low stability in CH_2Cl_2, even under an inert atmosphere. Compounds **1** and **2** appear to be extremely air-sensitive in solution, leading to black solutions upon exposure. In the solid state, all PMe_3-containing compounds **3**−**6** may be handled in air for short periods of time. In solution, they are readily oxidized by air to yield $WOCl_2(PMe_3)_3$[11] as one of the decomposition products.

Spectroscopy. The infrared spectra of *trans*-$W_2Cl_4(NHR)_2(NH_2R)_2$ (**1** and **2**) both exhibit characteristic ν(NH) in the range 3225−3325 cm^{-1}, as well as $\delta(NH_2)$ at 1563 (for **1**) and 1551 (for **2**) cm^{-1}, corresponding to the coordinated NH_2R and NHR ligands. Compounds **3**−**6** also show absorption bands in the IR spectra due to ν(NH) above 3000 cm^{-1}. The presence of NHR ligands in **1**−**6** is discernible from the ^{1}H NMR signals within the short range δ 11.84−12.53. In the cases of **1** and **2**, their ^{1}H NMR spectra give an AB pattern due to the diastereotopic NH_2 protons of the coordinated NH_2R groups with δ_A 3.65, δ_B 4.46 (for **1**) and δ_A 3.08, δ_B 3.69 (for **2**). However, the signals become broad due to coupling with the protons on adjacent R groups. Although the intermediate complexes **1** and **2** do not show molecular ion peaks M^+ and any other W_2-containing fragment ions in their FAB mass spectra, the corresponding PMe_3 substitution products display mass spectral peaks assignable to parent ions as well as fragment ions produced by sequential loss of amido, chlorine, and PMe_3 ligands.

The $^{31}P\{^1H\}$NMR spectra of *trans*- and *cis*-$W_2Cl_4(NHCy)_2(PMe_3)_2$ in C_6D_6 are depicted in Figure 2. Each of the spectra is characterized by a strong central singlet flanked by weak satellites due to $^{183}W-^{31}P$ coupling. The data, together with those of $W_2Cl_4(NHBu^s)_2(PMe_3)_2$, are collected in Table 3. Because of the stronger trans influence of NHR ligands compared to Cl ligands, the P−W bonds are notably stronger (*i.e.*, shorter as shown later) in the *cis* than in the *trans* isomer. The corresponding $^1J_{W-P}$ values are about 300 vs 110 Hz for the *cis* isomer vs the *trans* isomer. Also, the appearance of the satellites as doublets in the *cis* isomers usually serves as a useful indicator for identifying this kind of isomer in such systems. For an ABX spin system, PP^{183}W, the splitting observed in the satellites is proportional to J_{A-B} (*i.e.*, $^3J_{P-P}$ in such cases), and the $^3J_{P-P}$ values lie in the range 5−6 Hz. For the *cis* isomers, the P−P coupling constants are large enough to lead to a resolved splitting of the satellites, and approximate $^3J_{P-P}$ values may be readily obtained from the spectra. Obviously, from Table 3, the chemical shift and coupling constant parameters show little dependence on the identities of the amido ligands in these two cases.

(11) Chiu, K. W.; Lyons, D.; Wilkinson, G. *Polyhedron* **1983**, *2*, 803.

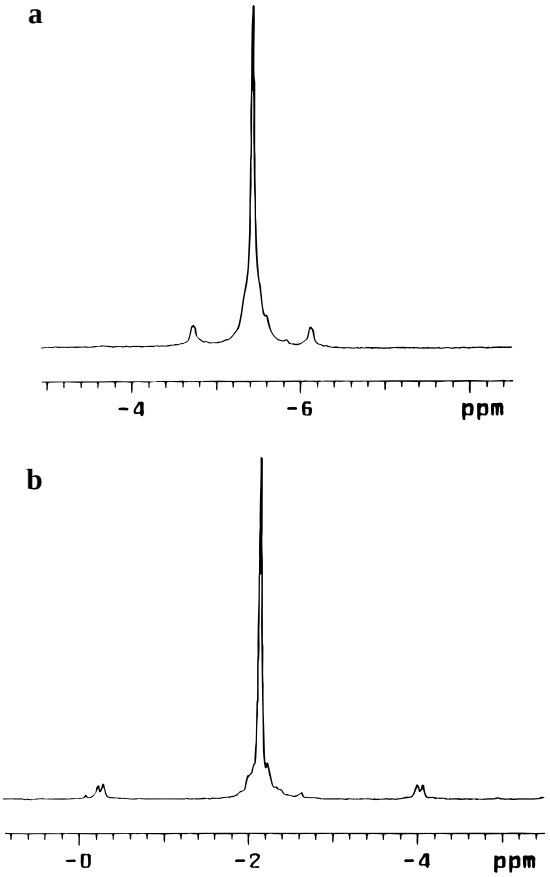

Figure 2. $^{31}P\{^1H\}$NMR spectra of (a) *trans*- and (b) *cis*-$W_2Cl_4(NHCy)_2(PMe_3)_2$ at room temperature in C_6D_6.

Table 3. ^{31}P NMR Data for the *Trans* and *Cis* Isomers of the $W_2Cl_4(NHR)_2(PMe_3)_2$ Compounds at Room Temperature

	trans		cis		
R	^{31}P shift[a]	$^1J_{W-P}$[b]	^{31}P shift	$^1J_{W-P}$	$^3J_{P-P}$
Bu^s	−5.30	116	−2.18	308	5.2
	−5.21	116	−2.15	308	5.2
Cy	−5.37	113	−1.89	308	5.0

[a] Relative to 85% H_3PO_4/D_2O in C_6D_6. [b] In hertz.

Another noteworthy feature is observed in the $^{31}P\{^1H\}$NMR spectra of *trans*- and *cis*-$W_2Cl_4(NHBu^s)_2(PMe_3)_2$, as shown in Figure 3. The *trans* isomer gives two closely spaced but separable signals of equal intensities with $\Delta(\delta)$ 0.03 ppm. Also, two sets of satellites are observed. Based on the fact that *RR*/*SS* and *RS*/*SR* configurations (*R* and *S* represent *R* and *S* configurations of the *sec*-butyl groups) of the *sec*-butyl groups are not mirror images but diastereoisomers, one signal probably arises from W_2R_2 and W_2S_2 molecules, while the other is caused by *RS* and *SR* configurations (W_2RS and W_2SR) in the W_2 units. In addition, the intensities of the NMR signals are expected to be equal in this case since the proportions of *RR*/*SS* and *RS*/*SR* should be 50:50 on a statistical basis. For *cis*-$W_2Cl_4(NHBu^s)_2(PMe_3)_2$, the corresponding spectrum again shows two close central peaks but with unequal intensities. This is presumably due to the preferential crystallization of one isomer with a particular configuration (*RR*/*SS* or *RS*/*SR*) over the other.

Isomerization and Kinetics. $^{31}P\{^1H\}$NMR spectroscopic studies showed that all the compounds of the *trans*-$W_2Cl_4(NHR)_2(PMe_3)_2$ type we have studied here undergo isomerization to produce the corresponding *cis*-$W_2Cl_4(NHR)_2(PMe_3)_2$ isomers in solution at room temperature. However, no evidence of isomerization back from a *cis* isomer to a *trans* isomer was observed for these new compounds, and thus it must be concluded that the equilibrium ratio, *cis*/*trans*, is very high. The isomerization process was followed as a function of time at 40 ± 1 °C by measuring the integrated intensities of the ^{31}P NMR signals arising from *trans* and *cis* isomers of $W_2Cl_4(NHCy)_2(PMe_3)_2$ (Figure 4). The results of a run for the trans-to-cis conversion of $W_2Cl_4(NHCy)_2(PMe_3)_2$ in toluene/C_6D_6 are shown graphically in Figure 5a. It can be seen that, in contrast to the behavior of the $W_2Cl_4(NHCMe_3)_2(PR_3)_2$ molecules,[2] no equilibrium is reached in this case and complete conversion to the *cis* isomer occurs eventually. Based on first-order kinetics, the rate constant for the trans → cis process is estimated to be 10(1) × 10^{-3} min^{-1} (Table 4). During the conversion experiment, there is usually some unavoidable decomposition to $W_2Cl_4(PMe_3)_4$,[2] which accounts for a slight decrease in the total intensity in Figure 5.

On the other hand, for the internal flip mechanism (or any other unimolecular mechanism) previously proposed[2] to be valid, the rate of isomerization would be expected to be insensitive to the presence of excess free PMe_3 ligand. As before, quantitative experimental tests have been carried out relating

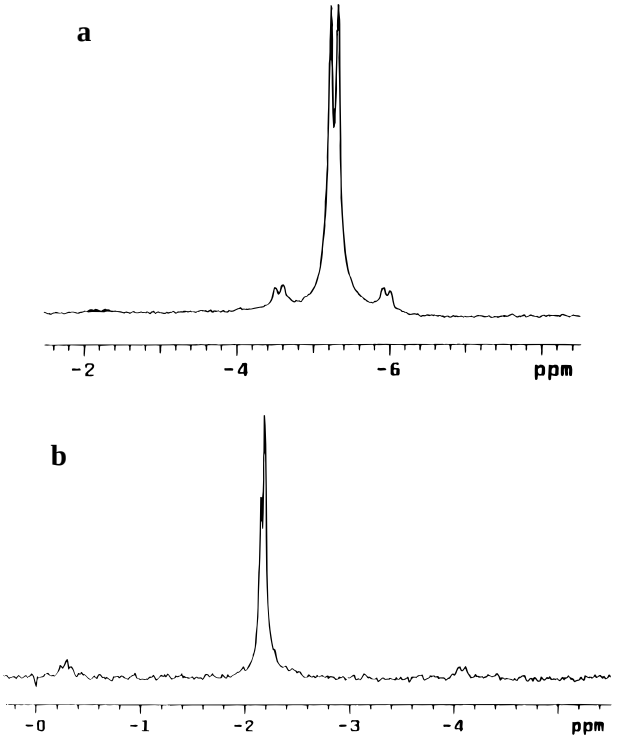

Figure 3. $^{31}P\{^1H\}$NMR spectra of (a) (±)-*trans*- and (b) (±)-*cis*-$W_2Cl_4(NHBu^s)_2(PMe_3)_2$ at room temperature in C_6D_6.

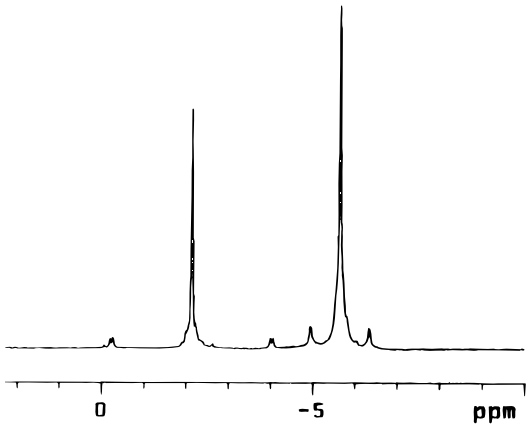

Figure 4. $^{31}P\{^1H\}$NMR spectrum of *trans*-$W_2Cl_4(NHCy)_2(PMe_3)_2$ after the sample was heated to 40 °C in C_6D_6/toluene for 1 h.

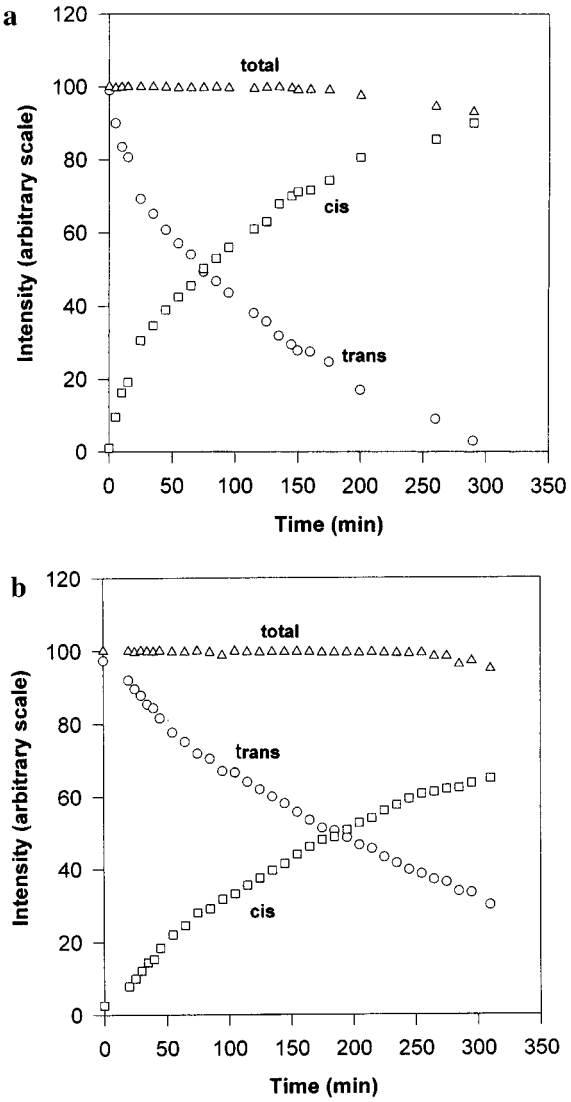

Figure 5. Graphs of the intensity of *trans*- and *cis*-$W_2Cl_4(NHCy)_2(PMe_3)_2$ vs time at 40 °C in C_6D_6/toluene (a) without free PMe_3 ligand and (b) with 0.01 M PMe_3.

Table 4. Rate Constants for the *trans*- to *cis*-$W_2Cl_4(NHCy)_2(PMe_3)_2$ Isomerizations at 40 °C

$[PMe_3]$ (M)	10^3k (min^{-1})
0	10(1)
0.01	3.7(3)
0.20	5.0(3)
0.25	4.7(4)

to this point. As for the $W_2Cl_4(NHCMe_3)_2(PR_3)_2$ molecules, it was found that the initial addition of excess PMe_3 caused a slight decrease (by 2−3-fold) in the trans → cis isomerization rate, but the effect is a little smaller in this case relative to that in $W_2Cl_4(NHCMe_3)_2(PR_3)_2$ compounds (about 4-fold decrease).[2] Figure 5b shows a plot of this run in the presence of 0.01 M PMe_3. The reaction rate was determined using a first-order rate law. A plot of $\ln(A_0/A_t)$ vs time is shown in Figure 6, where A_0 and A_t are the concentrations of *trans*-$W_2Cl_4(NHCy)_2(PMe_3)_2$ initially and at time *t*, respectively. It is apparent that the data points can be fitted to a straight line with correlation coefficient of 0.9981. The slope of the linear regression line corresponds to the rate constant for the isomerization process, and it was calculated to be $3.7(3) \times 10^{-3}$ min^{-1} (Table 4).

However, complications again arise when free PMe_3 concentrations continue to increase in the mixture. Table 4 summarizes the kinetic results concerning the effect of successive additions of PMe_3 on the rate constants for the trans → cis isomerization. After an approximately 2-fold decrease in rate upon addition of 0.01 M PMe_3, the rate did not show any further persistent decrease but remained rather constant over a range of $[PMe_3]$ from 0.01 to 0.25 M.

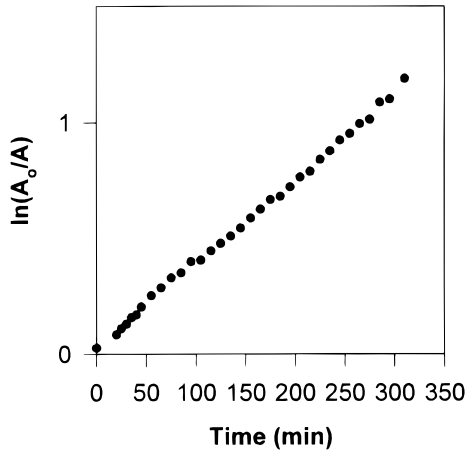

Figure 6. Plot of $\ln(A_0/A_t)$ vs time for trans → cis isomerization of $W_2Cl_4(NHCy)_2(PMe_3)_2$ at 40 °C in the presence of 0.01 M PMe_3.

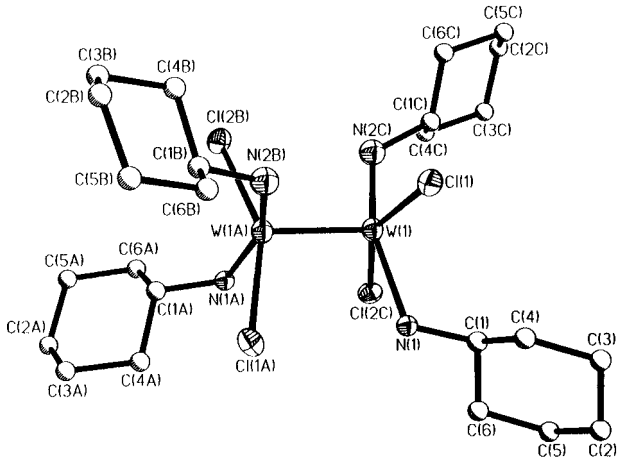

Figure 7. Perspective drawing of *trans*-$W_2Cl_4(NHCy)_2(NH_2Cy)_2$ (**2**). W and Cl atoms are represented by thermal ellipsoids at the 40% probability level. Carbon and nitrogen atoms are shown as spheres of arbitrary radius.

The interpretation of these observations has previously been discussed for $W_2Cl_4(NHCMe_3)_2(PR_3)_2$ molecules.[2] Generally speaking, competing mechanisms, one involving PMe_3 dissociation as the rate-determining step and the other a unimolecular (probably internal flip) mechanism, are suggested to explain the observed cis−trans isomerization processes. If we therefore treat the internal flip process as the second mechanism, with a rate of *ca.* 4.5×10^{-3} min^{-1} at 40 °C (*i.e.*, 7.5×10^{-5} s^{-1} at 313 K), the activation energy E_a for the rate-determining internal flip process can be estimated from the Arrhenius equation, $k = A\ e^{-E_a/RT}$, to be 25−29 kcal/mol, taking the pre-exponential factor as 10^{13}−10^{16}.

Molecular Structures. Compound **2** forms crystals in the noncentrosymmetric tetragonal space group $P\bar{4}2_1c$ with two molecules per unit cell. A perspective view of the molecule is depicted in Figure 7, and the key molecular parameters are given in Table 2. This compound provides only the second example of $W_2Cl_4(NHR)_2(NH_2R)_2$ molecules in an eclipsed geometry and a trans stereochemistry, the other being the *tert*-butylamido analog, $W_2Cl_4(NHCMe_3)_2(NH_2CMe_3)_2$.[3] A closely related intermediate complex in a cis configuration, $W_2Cl_4(NEt_2)_2$-

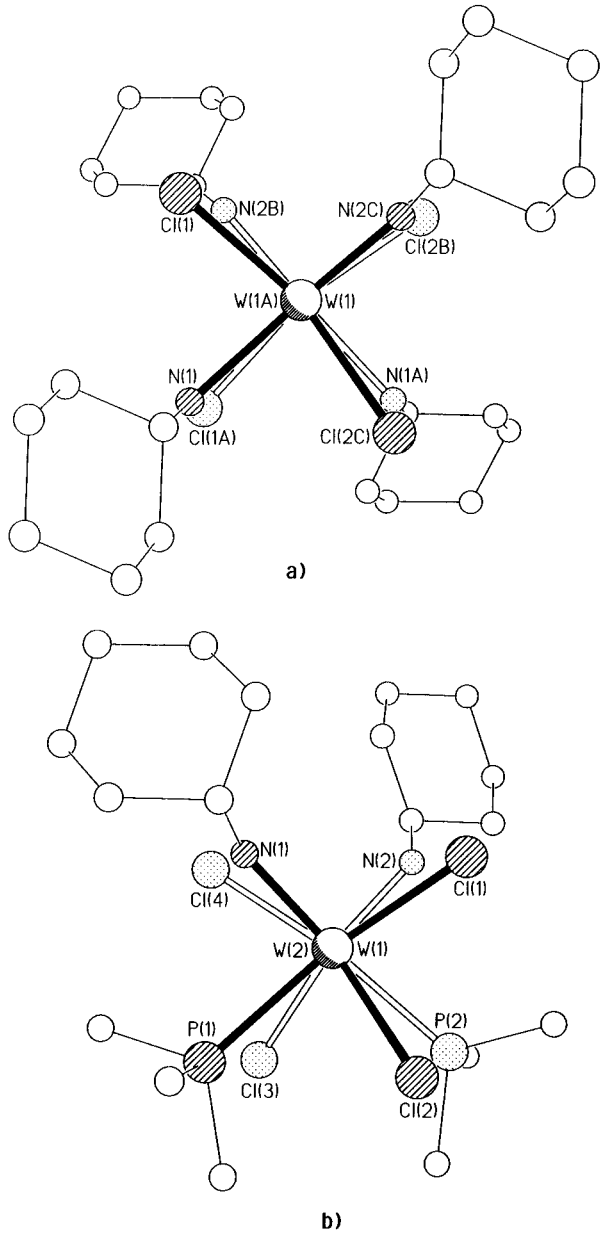

Figure 8. Views of (a) *trans*-$W_2Cl_4(NHCy)_2(NH_2Cy)_2$ (**2**) and (b) *cis*-$W_2Cl_4(NHCy)_2(PMe_3)_2$ **(6)** directly down the W−W axis. For clarity, carbon atoms are not labeled.

$(NHEt_2)_2$, has also been reported recently.[12] The molecular structure of **2** itself consists of two $WCl_2(NHCy)(NH_2Cy)$ fragments united by a W−W triple bond with the amide and amine groups trans to each other in each fragment. The two WCl_2N_2 units are eclipsed to each other, with nitrogen atoms opposite chlorine atoms (Figure 8a). The W−W bond distance of 2.2884(9) Å is very similar to that observed in $W_2Cl_4(NHCMe_3)_2(NH_2CMe_3)_2$ (2.288(3) Å) prepared by Bradley *et al.*[3] The present structure was initially solved and refined using a procedure similar to that adopted by Bradley *et al.*, in which the amide and amine groups were treated as the same unit without taking disordering into account. In this way, the unique W, N, and Cl atoms were located. All non-hydrogen atoms were refined with anisotropic thermal parameters. Again, as in the published structure for the *tert*-butyl analog, attempts to locate and refine the hydrogen atoms on N atoms were unsuccessful. The final refinement converged with $R = 0.029$ and $wR2 = 0.060$, and the corresponding selected bonding parameters are listed in Table 5. The W−N distance is 2.069(8) Å, which is midway between the normal distances for NHR (1.91(3) Å) and NH_2R (2.19(2)Å) groups in **2** (*vide infra*). Obviously, this model without separation of ligands yields molecular dimensions comparable to those of the reported structure, $W_2Cl_4(NHCMe_3)_2(NH_2CMe_3)_2$ (Table 5).

To surmount this problem, efforts were made to separate the ligands into two sets, which requires disordering of all the amide, amine, and Cl groups. This situation is best illustrated in Figure 9, which shows one tungsten fragment with two ligand sets. The atoms N(1) and N(2) correspond to the amino and amido nitrogens, respectively, and each of them, together with Cl(1) and Cl(2), was assigned a site occupancy factor (SOF) of 0.5. Atoms N(1) and N(1C), N(2) and N(2C), and so on are related by symmetry elements in space group $P\bar{4}2_1c$, so that the sum of SOF's equals 1 for each atom. In this way, we were able to distinguish the amine and amide groups from their distinctive W−N distances (W(1)−N(1), 2.19(2) Å; W(1)−N(2), 1.91(3) Å, respectively), which are in close agreement with the corresponding values observed in $W_2Cl_4(NEt_2)_2(NHEt_2)_2$ (2.198(7) and 1.908(7) Å)[12] (Table 5). Based on the knowledge already established in $W_2Cl_4(NEt_2)_2(NHEt_2)_2$ ($\angle Cl-W-N_{amide} > \angle Cl-W-N_{amine}$)[12] and *cis*-$W_2Cl_4(NHCy)_2(PMe_3)_2$ (*vide infra*) (Table 5), we assign Cl(1) and Cl(2C) as the corresponding chlorine atoms in the present model. The two W−Cl distances are comparable to each other in the resulting model.

In view of the successful refinement and reasonable resulting bond parameters using the separated ligand model, we decided to revisit the structure of $W_2Cl_4(NHCMe_3)_2(NH_2CMe_3)_2$[3] by the same approach. As expected, this new model affords bond distances and angles comparable to those in **2** (Table 5).

As far as the conformation of **2** is concerned, it maintains an eclipsed geometry due to the presence of intramolecular hydrogen bonding with small twist angles of 4.4 and 9.2°. The N(2C)−H···Cl(2B) and N(2B)−H···Cl(1) distances are both 2.46 Å.

Compounds **5** and **6** crystallize in the monoclinic space groups $P2_1/a$ and $P2_1/n$, respectively, with four molecules (constituting two enantiomeric pairs of molecules) per unit cell for each complex. Perspective views of the molecular structures of **5** and **6** are shown in Figures 10 and 11. In fact, we note that there are only two prior examples of this type of molecule in a cis configuration in the literature, namely *cis*-$W_2Cl_4(NHCMe_3)_2(PR_3)_2$ (R_3 = Me_3, Me_2Ph).[1,13] Both of the molecules **5** and **6** are chiral and have an idealized C_2 symmetry. The core structure, consisting of the set of eight ligands, is essentially the same in the two compounds. Each molecule possesses an effectively eclipsed geometry (Figure 8b), with its two WCl_2NP ligand sets arranged in a fashion akin to that encountered in the related W_2^{6+} complexes, *cis*-$W_2Cl_4(NHCMe_3)_2(PR_3)_2$ (R_3 = Me_3, Me_2Ph).[13] In all cases, each W atom of the $(W{\equiv}W)^{6+}$ center is four-coordinate, and the two chlorine atoms are in a cis arrangement in each W unit. In no case was disorder of the W_2 unit in the crystal encountered. The W−W bond distances are 2.320(1) and 2.3229(5) Å respectively for **5** and **6** (Table 6), which are consistent with a W−W triple bond with a $\sigma^2\pi^4$ ground state electronic configuration.[14] These distances do not vary significantly from those

(12) Cotton, F. A.; Dikarev, E. V.; Nawar, N.; Wong, W. Y. *Inorg. Chem.* **1997**, *36*, 559.

(13) Bradley, D. C.; Hursthouse, M. B.; Powell, H. R. *J. Chem. Soc., Dalton Trans.* **1989**, 1537.

(14) Cotton, F. A.; Walton, R. A. *Multiple Bonds between Metal Atoms*, 2nd ed.; Oxford University Press: New York, 1993; see also references therein.

Table 5. Distances (Å) and Angles (deg) in *trans*-$W_2Cl_4(NHR)_2(NH_2R)_2$ (R = Bu^t, Cy) and Related Compounds

	trans-$W_2Cl_4(NHCy)_2(NH_2Cy)_2$[a,c]	*trans*-$W_2Cl_4(NHCy)_2(NH_2Cy)_2$[b,c]	*trans*-$W_2Cl_4(NHBu^t)_2(NH_2Bu^t)_2$[b,3]	*trans*-$W_2Cl_4(NHBu^t)_2(NH_2Bu^t)_2$[a,c]	*cis*-$W_2Cl_4(NEt_2)_2(NHEt_2)_2$[12]	*cis*-$W_2Cl_4(NHCy)_2(PMe_3)_2$[c]
W−W	2.2884(9)	2.286(1)	2.288(3)	2.284(1)	2.3084(5)	2.3229(5)
W−N_{amine}	2.19(2)	2.069(8)	2.11(2)	2.24(2)	2.198(7)	
W−N_{amide}	1.91(3)	2.069(8)	2.11(2)	2.00(3)	1.908(7)	1.901(5), 1.907(5)
W−Cl	2.37(2), 2.38(1)	2.359(3)	2.352(5)	2.345(8), 2.388(8)	2.384(2), 2.473(2)	2.384(2), 2.393(2), 2.414(2), 2.421(2)
∠Cl−W−N_{amine}	84(1), 79.1(9)	89.4(4), 86.5(4)	89.0(5)	83.8(6), 82.8(6)	79.7(2)	
∠Cl−W−N_{amide}	97(1), 92(1)	89.4(4), 86.5(4)	89.0(5)	92(1), 93(1)	92.9(2)	96.5(2), 97.1(2)
∠W−N_{amine}−C	113(2)	120.3(6)	132(1)	131(2)	111.4(5), 117.9(5)	
∠W−N_{amide}−C	128(2)	120.3(6)	132(1)	135(3)	112.2(6), 135.6(6)	127.1(4), 120.5(6)

[a] Based on a model with separated amine and amide groups. [b] Based on a model without separation of amine and amide groups. [c] This work.

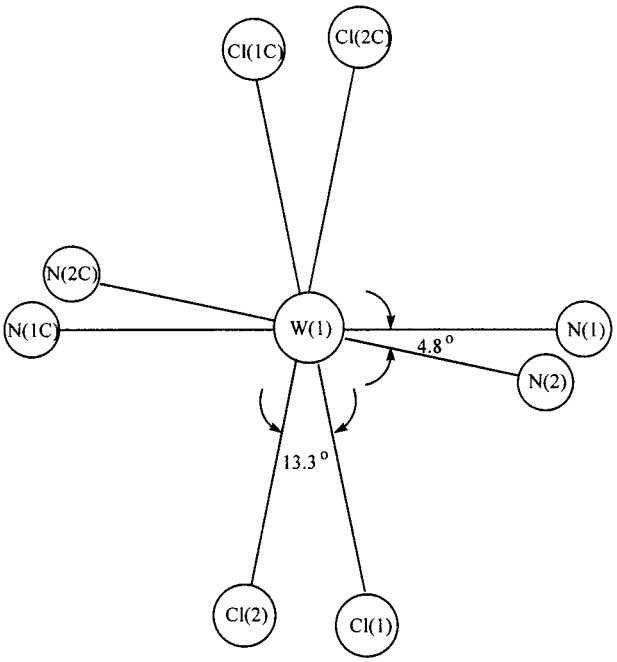

Figure 9. Schematic diagram showing the structural model for **2** with separated ligand sets in one W fragment.

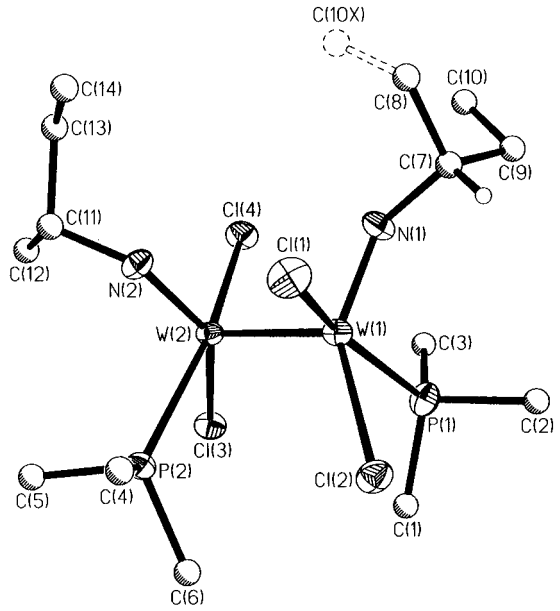

Figure 10. Perspective drawing of *cis*-$W_2Cl_4(NHBu^s)_2(PMe_3)_2$ (**5**). Some atoms are represented by thermal ellipsoids at the 40% probability level. Carbon atoms are shown as spheres of arbitrary radius. The disordered carbon atom C(10X) in one of the NHBu^s groups is shown.

observed in *cis*-$W_2Cl_4(NHCMe_3)_2(PMe_3)_2$ (2.3267(6) Å).[1,13] The average W−N bond distances of 1.89(1) Å in **5** and 1.904(5) Å in **6** represent normal W−NH(R) bond lengths of formal bond order 2. The mean W−P bond lengths for **5** and **6** are respectively 2.500(4) and 2.512(2) Å. The W−Cl distances trans to N are longer than those trans to P. This difference in W−Cl distances indicates that NHR groups exert a greater structural trans effect than the phosphines. In both **5** and **6**, there are two hydrogen bonds across the W−W triple bond (average N−H···Cl distance, 2.41 Å in **5** and 2.46 Å in **6**), and the mean torsion angles involving the hydrogen-bonded N and Cl atoms are 16.2 and 13.3° for **5** and **6**, respectively.

For **5**, another notable structural feature is that one of the coordinated NHR ligands exhibits disordered *sec*-butyl carbon atoms with equal occupancy of two sets of positions. Thus, three configurations are possible, namely W_2R_2, W_2RS, and W_2S_2, in the crystal lattice of **5** (*R* and *S* represent *R* and *S* configurations of the *sec*-butyl groups). In a separate X-ray diffraction experiment on another red-brown crystal from the same reaction, the structure analysis revealed that it also contains four molecules of *cis*-$W_2Cl_4(NHBu^s)_2(PMe_3)_2$ in a unit cell of comparable cell volume,[6] but the unit cell parameters are slightly different. In view of the fact that the two chiral carbon atoms of the *sec*-butyl moieties in the asymmetric unit adopt the same configuration (either *RR* or *SS*) in this case, we might expect that these two polymorphic forms give rise to different packing in the unit cells, which will lead to different lattice parameters. Since the same numbers of *R* and S centers exist in both cases, there is no racemization of Bu^s groups in the reaction products.

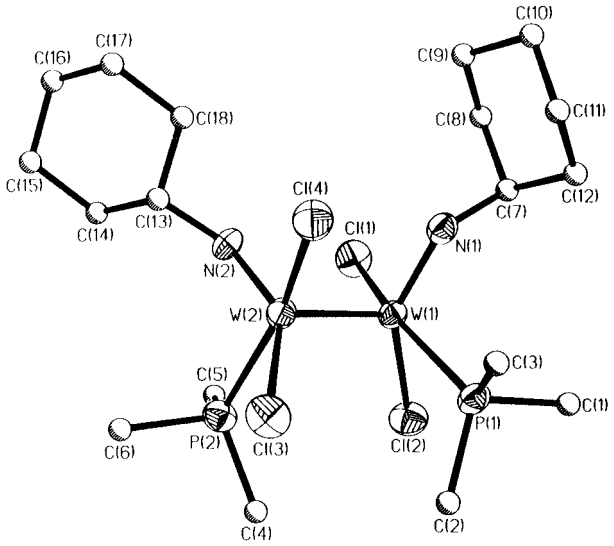

Figure 11. Perspective drawing of *cis*-$W_2Cl_4(NHCy)_2(PMe_3)_2$ (**6**). Atoms are represented by thermal ellipsoids at the 40% probability level. Carbon atoms are shown as spheres of arbitrary radius. Only the main orientation for the C(13)−C(18) cyclohexyl ring is displayed.

Table 6. Selected Bond Distances (Å) and Angles (deg) and Torsion Angles (deg) for *cis*-$W_2Cl_4(NHBu^s)_2(PMe_3)_2$ (**5**) and *cis*-$W_2Cl_4(NHCy)_2(PMe_3)_2$ (**6**)

	5	**6**
W(1)−W(2)	2.320(1)	2.3229(5)
W(1)−P(1)	2.487(4)	2.507(2)
W(2)−P(2)	2.513(3)	2.516(2)
W(1)−N(1)	1.88(1)	1.901(5)
W(2)−N(2)	1.90(1)	1.907(5)
W(1)−Cl(1)	2.370(3)	2.384(2)
W(2)−Cl(4)	2.383(3)	2.393(2)
W(1)−Cl(2)	2.424(3)	2.414(2)
W(2)−Cl(3)	2.419(3)	2.421(2)
P(1)−W(1)−N(1)	87.6(4)	88.0(2)
P(1)−W(1)−Cl(1)	159.1(1)	159.92(6)
P(1)−W(1)−Cl(2)	80.1(1)	79.21(6)
N(1)−W(1)−Cl(1)	96.5(4)	96.5(2)
N(1)−W(1)−Cl(2)	146.9(4)	145.0(2)
Cl(1)−W(1)−Cl(2)	85.6(2)	86.07(7)
W(2)−W(1)−P(1)	96.73(9)	95.85(4)
W(2)−W(1)−N(1)	97.4(3)	98.2(2)
W(2)−W(1)−Cl(1)	103.0(1)	102.80(5)
W(2)−W(1)−Cl(2)	114.3(1)	115.35(5)
P(2)−W(2)−N(2)	86.6(4)	88.1(2)
P(2)−W(2)−Cl(3)	79.9(1)	79.88(6)
P(2)−W(2)−Cl(4)	160.9(1)	160.62(7)
N(2)−W(2)−Cl(3)	145.0(4)	144.9(2)
N(2)−W(2)−Cl(4)	99.2(4)	97.1(2)
Cl(3)−W(2)−Cl(4)	85.2(1)	85.31(6)
W(1)−W(2)−P(2)	95.73(9)	95.85(4)
W(1)−W(2)−N(2)	97.1(4)	97.6(2)
W(1)−W(2)−Cl(3)	116.2(1)	116.22(5)
W(1)−W(2)−Cl(4)	101.53(9)	101.90(5)
P(1)−W(1)−W(2)−Cl(3)	19.3(1)	15.23(6)
N(1)−W(1)−W(2)−Cl(4)	17.4(4)	13.5(2)
Cl(1)−W(1)−W(2)−N(2)	14.9(4)	13.1(2)
Cl(2)−W(1)−W(2)−P(2)	18.7(1)	16.00(7)

Concluding Remarks

The preparation of $W_2Cl_4(NHR)_2(PMe_3)_2$ (R = Bu^s, Cy) molecules by reaction of $W_2Cl_4(NHR)_2(NH_2R)_2$-type intermediate complexes with PMe_3 is reported. It was shown by $^{31}P\{^1H\}$ NMR spectral data that the initial products are pure *trans* isomers, but these compounds readily isomerize in an irreversible manner to the *cis*-C_2 isomers (see Figure 1). In a future article, results concerning our continuing efforts in the search of the unknown *cis* isomer (*cis*-C_i) by using the least sterically bulky amide ligands will be presented.

Perhaps one of the most interesting aspects here is the structural characterization of *trans*-$W_2Cl_4(NHCy)_2(NH_2Cy)_2$, in which the disordering of the ligands around W atoms due to the difference in amine and amide groups is carefully studied and formulated. The earliest example of this type of molecule was the analogous compound *trans*-$W_2Cl_4(NHCMe_3)_2(NH_2CMe_3)_2$ reported by Bradley et al.[3] While there was surely no reason to doubt that this compound had been correctly formulated, the crystallographic support for the structure itself was a bit troubling in that both amide and amine ligands were refined as a single group, leading to a W−N distance of 2.11(2) Å. Our successful resolution of the ligand sets in **2** opened the possibility of reexamining the structure of $W_2Cl_4(NHCMe_3)_2(NH_2CMe_3)_2$. An analogous form of disorder was shown to exist in $W_2Cl_4(NHCMe_3)_2(NH_2CMe_3)_2$, and, with separation of the ligands, reasonable molecular dimensions are obtained. It would appear that such a disorder is likely to occur in all compounds of the *trans*-$W_2Cl_4(NHR)_2(NH_2R)_2$ type, but, when the structure is refined so that this is included in the model, entirely satisfactory molecular dimensions are obtained.

Acknowledgment. We thank the National Science Foundation for support.

Supporting Information Available: Three X-ray crystallographic files, in CIF format, are available. Access information is given on any current masthead page.

IC961485O